Many-Wavelength Interferometry with Thousands of Lasers for Absolute Distance Measurement

S. A. van den Berg,* S. T. Persijn, and G. J. P. Kok
National Metrology Institute VSL, Thijsseweg 11, 2629 JA Delft, The Netherlands

M. G. Zeitouny and N. Bhattacharya
Technische Universiteit Delft, Lorentzweg 1, 2628 CJ Delft, The Netherlands
(Received 6 December 2011; published 1 May 2012)

We demonstrate a new technique for absolute distance measurement with a femtosecond frequency comb laser, based on unraveling the output of an interferometer to distinct comb modes with 1 GHz spacing. From the fringe patterns that are captured with a camera, a distance is derived by combining spectral and homodyne interferometry, exploiting about 9000 continuous wave lasers. This results in a measurement accuracy far within an optical fringe ($\lambda/30$), combined with a large range of nonambiguity (15 cm). Our technique merges multiwavelength interferometry and spectral interferometry, within a single scheme.

DOI: 10.1103/PhysRevLett.108.183901 PACS numbers: 42.79.Pw, 06.30.Bp, 07.60.Ly, 42.62.Eh

Optical distance measurement is one of the fields that has been influenced significantly by the advent of the femtosecond frequency comb [1–4]. By connecting the optical and microwave domain of the electromagnetic spectrum, the frequency comb provides a straight relation between the meter and the second. These two SI base units have been connected since 1983, when the speed of light in vacuum was defined to be exactly equal to $c = 299\,792\,458$ m/s. Formally, the meter is defined as the distance traveled in vacuum in $1/c$ seconds. In practice the meter is usually realized with a wavelength-stabilized laser, which is calibrated by measuring its optical frequency with respect to a time standard like a Cs atomic clock. The frequency comb has tremendously simplified these measurements compared to earlier work where a phase coherent frequency chain was used [5]. However, the frequency comb is not only applied for calibration of continuous wave lasers that are used for distance measurement [6,7], but it is also exploited as a distance measurement tool itself. One of the first distance measurements with the comb was based on synthetic wavelength generation using the high harmonics of the repetition frequency within the comb bandwidth [8]. Other schemes rely on optical interferometry based on cross-correlation between pulses emitted by the frequency comb laser [9–11], spectral (dispersive) interferometry [12,13], or multiheterodyne interferometry using two frequency combs with a slightly different repetition frequency [14,15]. A noninterferometric approach based on time-of-flight measurements has also been reported [16].

In this Letter we demonstrate the measurement of an arbitrary absolute distance with a mode-resolved frequency comb laser. The output of a Michelson interferometer is analyzed with a high resolution spectrometer based on a virtually imaged phase array (VIPA) and a grating [17,18]. The VIPA spectrometer shows an unprecedented resolution, unraveling the 1 GHz spaced comb frequencies to distinct modes. This allows for visualizing interference of frequency comb light on the individual mode level. The distance is determined from both spectral interferometry and massively parallel homodyne interferometry of about 9000 frequency comb modes. This new technique can be considered as a combination of multiwavelength interferometry with thousands of continuous wave lasers and spectral (dispersive) interferometry. It overcomes the limitations of the individual techniques, combining an interferometric scheme with a large range of nonambiguity. This allows for nonincremental absolute measurement of an arbitrary distance with a single frequency comb laser. The measurement range is only fundamentally limited by the comb linewidth, essentially permitting distance measurements up to thousands of kilometers.

The femtosecond frequency comb laser we operate is a Ti:Sapphire oscillator with a repetition rate of 1 GHz, emitting pulses of about 40 fs. The repetition rate, f_{rep}, and the carrier-envelope offset frequency, f_0, are stabilized to a cesium atomic clock, with a relative accuracy of about 10^{-12} in 1 s. The comb light is coupled into a single-mode fiber to deliver about 4 mW of light to a Michelson interferometer with a clean beam profile. A schematic overview of the setup is shown in Fig. 1. The Michelson interferometer consists of a fixed reference arm and a measurement arm with a travel range of 15 cm spanning the pulse-to-pulse distance L_{pp} (30 cm). The interferometer output is analyzed with a spectrometer, based on a virtually imaged phase array [17,19] and a grating [18,20]. The VIPA has a free spectral range of 50 GHz. Because of the highly reflective coatings ($> 99.94\%$ and 99.5%), the frequency comb modes are fully resolved. For our comb laser within a bandwidth of 808–828 nm, about 9000 modes are present, which are captured within one image of a charge-coupled device (CCD) camera. We use an

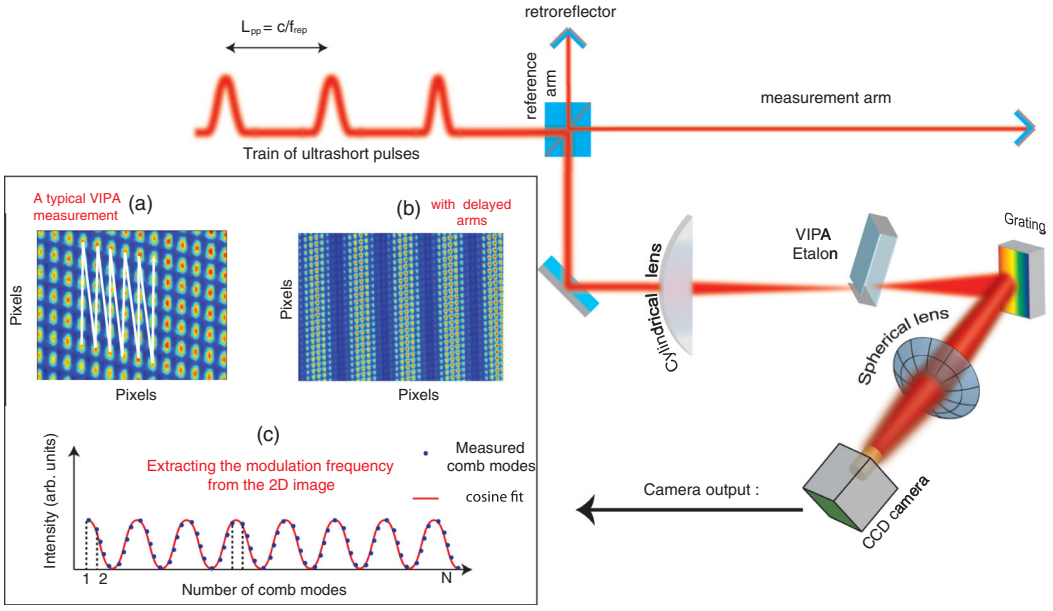

FIG. 1 (color online). Schematic overview of the setup for unraveling the output of a Michelson interferometer into distinct modes. In the inset (a) a small fraction of a typical CCD image is shown, as obtained with the measurement path blocked. Inset (b) shows a part of the CCD image when interference between the two arms occurs. The mode-resolved signal is mapped on a frequency axis by stitching together vertical lines, as schematically indicated by the white arrows (in reality one vertical line consists of about 50 dots). The result is shown in (c).

acquisition time of 100 ms here, but since only a small fraction (about 2%) of the available laser power is used, shorter acquisition times can be chosen if required. In the inset of Fig. 1, a part of a typical CCD image is shown, as taken with the measurement arm blocked (a). When both paths are unblocked, interference between each mode and itself occurs, which can be seen in Fig. 1(b).

We have measured spectral interference for several path length differences between measurement and reference arm. Typical pictures are shown in Fig. 2. In Fig. 2(a) the delay between the arms is small (33 μm), leading to only a few fringes within the comb bandwidth. However, for longer delay the high resolution provided by the VIPA is essential for resolving the interference pattern, showing dark and light spots along one vertical line. Examples are shown Figs. 2(b) and 2(c), with a delay of 2.5 and 20 mm, respectively. In Fig. 2(d) the delay is set at $L_{pp}/4$ (73.9 mm), with L_{pp} the pulse-to-pulse distance $L_{pp} = c/nf_{\mathrm{rep}}$. Here c is the speed of light in vacuum and n the refractive index of air. In this case the pulse separation is at its maximum value. In the spectral domain this leads to alternating dark and light dots; i.e., the phase difference between neighboring modes equals π. Figure 2(e) shows the pattern at 110 mm. For a distance approaching $L_{pp}/2$, consecutive pulses start overlapping and the phase difference between neighboring lines approaches 2π [Fig. 2(f)].

We use an algorithm to identify the position of the dots on the image. The power of each dot is determined by taking the integrated value of 5×5 pixels, largely covering an individual dot. Since the illumination of the CCD chip by the VIPA interferometer is not entirely homogeneous, these values are normalized on reference values, as obtained with one of the interferometer arms closed. The frequency calibration of the individual dots on the camera is performed with an optical parametric oscillator (OPO). The OPO output is tuned to a wavelength within the comb bandwidth and brought to the spectrometer via the same fiber as the comb source for perfect overlap of the beam path. In parallel, the OPO output is measured with a wave meter with an absolute accuracy of several tens of megahertz. This is repeated at several wavelengths within the comb bandwidth, providing the optical frequency of each dot. Each vertical line contains about 50 unique frequencies, as determined by the free spectral range of the VIPA. These unique frequencies of neighboring vertical lines are stitched together such that the two-dimensional image is mapped onto a calibrated frequency scale. As an example, the unwrapped spectral interferometry data for delays of 33 μm and 2.5 mm are displayed in Fig. 3.

An absolute distance is derived from the spectral interferometry measurements by determining the phase change as a function of optical frequency. The interference term describing the output of the Michelson interferometer is proportional to $\cos\phi$. If dispersion is negligibly small, as in our case, the optical phase $\phi = 4\pi Lnf/c$ depends linearly on the optical frequency f and L. Here L is the one-way path length difference of the interferometer. This allows for a cosine fit through the measurement data to determine

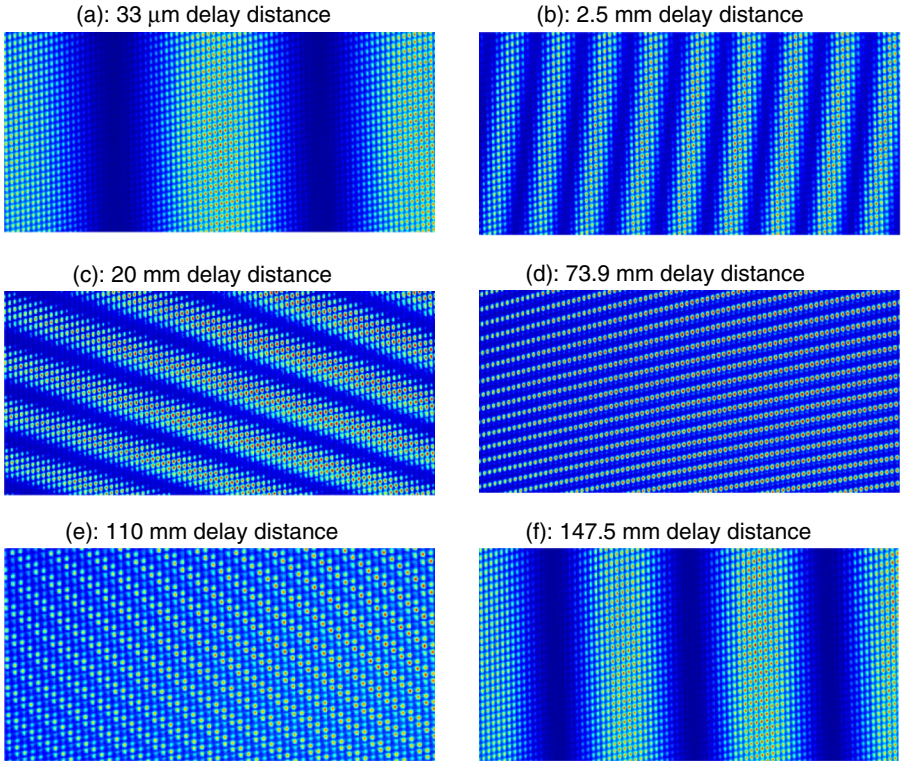

FIG. 2 (color online). Measurements obtained with the VIPA interferometer for various delays between measurement and reference path. Images (a), (b), and (c) are taken at a delay of 33 μm, 2.5 mm, and 20 mm, respectively. Image (d) shows the case of maximum pulse separation, which occurs at $L_{pp}/4 = 73.9$ mm, showing π phase difference between neighboring comb modes. Images (e) and (f) are taken at a delay of 110 mm and 147.5 mm, respectively. For clarity only a quarter of the total CCD chip area is shown.

$L = cP_{\mathrm{mod}}/(4\pi n)$, with the modulation parameter $P_{\mathrm{mod}} = 4\pi Ln/c = d\phi/df$ obtained from the curve fit. The modulation parameter is equivalent to the slope of the unwrapped phase, as obtained from methods based on fast Fourier transform [12,13]. The resolved comb frequencies are markers with a constant separation equal to the repetition rate of the laser. Therefore, the dots provide a frequency scale with a relative uncertainty of 10^{-12}. This is a huge advantage compared to lower resolution spectral interferometry, which requires careful calibration of the frequency axis [13]. Furthermore, the measurement range is not limited to a certain maximum pulse separation here. Since the comb spectrum is entirely resolved, a signal is obtained, even at maximum separation of the pulses. Note

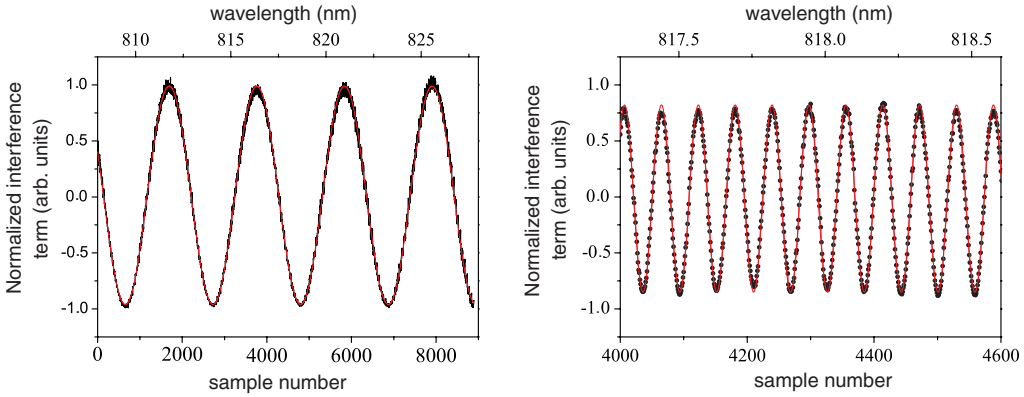

FIG. 3 (color online). The unraveled comb, with the frequency samples stitched together along the frequency axis. The frequency of a single dot is obtained from $f(p) = f_{\mathrm{rep}}(Q - p) + f_0$, with p the sample number, Q an integer equal to 365 457, as determined by the frequency calibration, $f_{\mathrm{rep}} = 1014.82$ MHz and $f_0 = -180$ MHz. Left: delay of 33 μm. Right: delay of 2.5 mm, zoomed to a fraction of the full scale for clarity. The individual samples are indicated by black dots. The solid (red) curves represent a cosine fit through the data.

that since the distance is only determined from the slope $d\phi/df$, the absolute optical frequency of the dots and the offset frequency f_0 have not been required so far.

By also considering the absolute frequency of each dot, the distance measurement can be refined. Each comb line can be considered a continuous wave laser, allowing for massively parallel homodyne interferometry with thousands of lasers within the comb bandwidth. For each mode (labeled i) the distance L_i is calculated from $L_i = (m_i + \phi_i/2\pi)\lambda_i/(2n_i)$ for a wavelength λ_i and a corresponding refractive index n_i. The integer number of wavelengths m_i is determined from the previous measurement based on spectral interferometry. The phase for the specific wavelength λ_i, ϕ_i, is found from the cosine fit. This way of determining the phase at a certain wavelength is not sensitive to intensity variations, as is the case of homodyne interferometry with a single wavelength. For each comb wavelength a distance is determined. A final value for the distance is obtained by averaging the values as found for each comb wavelength.

We validate our measurements by comparing them to a fringe-counting wavelength-stabilized helium-neon (HeNe) laser for several distances within the scanning range of the interferometer. The HeNe laser is coupled into the measurement arm of the Michelson interferometer via a dichroic mirror, transmitting the helium-neon light at 633 nm and reflecting the comb light at 820 nm. For each position the fringe pattern is analyzed using the combined method described above. Since the HeNe laser only measures incrementally, one fringe pattern is recorded at a starting point close to zero delay, giving the one-way path length difference L_0. After displacement a second picture is recorded, providing the displacement $\Delta L = L - L_0$. The comparison between HeNe and comb measurements is plotted in Fig. 4. Averaged over all displacements measured, the difference between HeNe and comb method is about 8 nm, with a standard deviation of 28 nm ($\lambda/30$), indicating that statistical variations dominate the comparison measurement. Since the HeNe laser and the frequency comb have only the measurement path in common, limited interferometer stability and air fluctuations contribute to the difference and variation on these measurements. The measurement uncertainty of the HeNe laser is estimated to be 10–20 nanometers. The relative uncertainty on the determination of the modulation parameter (or phase), resulting from the curve fit, directly determines the relative uncertainty on the spectral interferometry measurement. This is not the case in the homodyne scheme, where the uncertainty on the phase only affects the phase fraction to be added to the integer m_i. The measurement uncertainty for a homodyne measurement is indicated as error bars in Fig. 4, ranging from a few to tens of nanometers, depending on the pulse separation. When measuring longer distances, e.g., hundreds of pulse-to-pulse distances, f_{rep} may be chosen such that pulse separation is small and only a few fringes are observed within the comb bandwidth. In this way the measurement uncertainty resulting from the phase determination can be minimized.

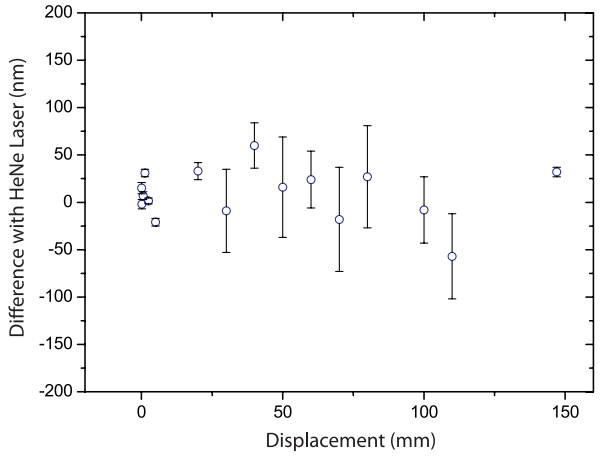

FIG. 4 (color online). Comparison between comb-based distance measurements using the VIPA spectrometer and a counting HeNe laser. The uncertainty bars represent the uncertainty on a homodyne measurement, resulting from the uncertainty on the cosine fit.

As discussed above, the pulses have maximum separation at $L_{pp}/4$. In this case the fastest spectral modulation occurs, where dark and light dots alternate. In case of white light interferometry with a continuous spectrum, the spectral modulation would always increase with distance. Because of the finite number of samples (comb lines), the Nyquist theorem applies here. For distances exceeding $L_{pp}/4$ a case of undersampling occurs, resulting in decreasing spectral modulation. A slight change of f_{rep} can be used to determine whether the distance is above or below $L_{pp}/4$. At a distance of $L_{pp}/2$, the total path length difference equals the pulse-to-pulse difference. In this case, the phase difference between neighboring comb lines equals 2π. Here all frequency components have the same phase, but this does not occur at a coherence maximum. Since f_0 is not equal to 0, all frequency components have the phase $2\pi f_0/f_{\mathrm{rep}}$. For distances exceeding $L_{pp}/2$, the fringe pattern starts repeating. For longer distances the integer number of $L_{pp}/2$ thus needs to be known, requiring a course determination of the distance with an accuracy within the range of nonambiguity of 15 cm. This is a rather loose requirement compared to single wavelength interferometry, requiring a course measurement within $\lambda/2$. A measurement of the distance within 15 cm, can be obtained with, e.g., time-of-flight measurement or by changing f_{rep}.

We have visualized interferometry with a frequency comb laser on the level of individual modes, by unraveling the output of a Michelson interferometer with a VIPA spectrometer. Interference patterns are captured within a single camera shot, containing a wealth of distance

information. A distance is measured by combining spectral interferometry and homodyne interferometry with thousands of wavelengths. This results in an agreement within $\lambda/30$, in comparison to a fringe-counting interferometer. The presented approach combines interferometry with a long range of nonambiguity, allowing for nonincremental distance measurement. The measured distance can be extended to a longer range, possibly to thousands of kilometers in vacuum conditions, which may be of interest for space applications, like distance measurement between satellites. Another application may be the determination of refractive index and dispersion of materials.

This work is part of EURAMET joint research project "Absolute Long Distance Measurement in Air" and has received funding from the European Community's Seventh Framework Programme, ERA-NET Plus, under Grant Agreement No. 217257.

*svdberg@vsl.nl

[1] D. J. Jones, S. A. Diddams, J. K. Ranka, A. Stentz, R. S. Windeler, J. L. Hall, and S. T. Cundiff, Science **288**, 635 (2000).
[2] R. Holzwarth, Th. Udem, T. W. Hänsch, J. C. Knight, W. J. Wadsworth, and P. St. J. Russell, Phys. Rev. Lett. **85**, 2264 (2000).
[3] N. R. Newbury, Nature Photon. **5**, 186 (2011).
[4] S.-W. Kim, Nature Photon. **3**, 313 (2009).
[5] H. Schnatz, B. Lipphardt, J. Helmcke, F. Riehle, and G. Zinner, Phys. Rev. Lett. **76**, 18 (1996).
[6] T. Yoon, J. Ye, J. Hall, and J.-M. Chartier, Appl. Phys. B **72**, 221 (2001).
[7] Y. Salvadé, N. Schuhler, S. Lévêque, and S. Le Floch, Appl. Opt. **47**, 2715 (2008).
[8] K. Minoshima and H. Matsumoto, Appl. Opt. **39**, 5512 (2000).
[9] J. Ye, Opt. Lett. **29**, 1153 (2004).
[10] M. Cui, M. G. Zeitouny, N. Bhattacharya, S. A. van den Berg, H. P. Urbach, and J. J. M. Braat, Opt. Lett. **34**, 1982 (2009).
[11] P. Balling, P. Křen, P. Mašika, and S. A. van den Berg, Opt. Express **17**, 9300 (2009).
[12] K.-N. Joo, Y. Kim, and S.-W. Kim, Opt. Express **16**, 19799 (2008).
[13] M. Cui, M. G. Zeitouny, N. Bhattacharya, S. A. van den Berg, and H. P. Urbach, Opt. Express **19**, 6549 (2011).
[14] I. Coddington, W. C. Swann, L. Nenadovic, and N. R. Newbury, Nature Photon. **3**, 351 (2009).
[15] T.-A. Liu, N. R. Newbury, and I. Coddington, Opt. Express **19**, 18501 (2011).
[16] J. Lee, Y.-J. Kim, K. Lee, S. Lee, and S.-W. Kim, Nature Photon. **4**, 716 (2010).
[17] S. Xiao and A. Weiner, Opt. Express **12**, 2895 (2004).
[18] S. A. Diddams, L. Hollberg, and V. Mbele, Nature (London) **445**, 627 (2007).
[19] M. Shirasaki, Opt. Lett. **21**, 366 (1996).
[20] M. J. Thorpe, D. Balslev-Clausen, M. S. Kirchner, and J. Ye, Opt. Express **16**, 2387 (2008).